Combined Wideband Channel Estimation and Direct Link Interference Mitigation in Bistatic Backscatter Systems

Lukas D'Angelo*†, Benjamin J. B. Deutschmann*, Klaus Witrisal*†
*Graz University of Technology, Graz, Austria, †Christian Doppler Laboratory for Location-aware Electronic Systems
email: {lukas.dangelo, benjamin.deutschmann, witrisal}@tugraz.at

***Abstract*—In this paper, we present a novel algorithm for simultaneous direct link interference (DLI) mitigation and channel state information (CSI) estimation in wideband single-input single-output (SISO) backscatter (BS) systems. First, we establish a time-domain signal model to derive a method to separate the weak backscatter signal from the strong DLI by exploiting the masking property of the binary on–off keying (OOK) modulation of the backscatter device. Based on the time-domain model, we derive an estimator for the unknown parameters of the OOK modulation signal, which incorporates inherent cancellation of the direct link signal. With the obtained estimate of the modulation parameters, the impulse responses of the DLI and BS channels are estimated, using a masked maximum likelihood approach. The obtained algorithm is evaluated using a standard-compliant orthogonal frequency-division multiplexing (OFDM) transmission for the interrogation system and a radio frequency identification (RFID) preamble for the BS modulation. Exploiting the inherent spreading gain due to the wideband OFDM signal, we are able to recover the parameters of the BS signal at an SNR as low as -20 dB. Furthermore, we perform a proof-of-concept measurement in a wired BS setup using a pseudo-noise transmit signal and use the received signal to test the obtained algorithm.**

***Index Terms*—Bistatic backscatter communication, interference mitigation, OFDM, RFID**

I. Introduction

With the vastly increasing number of interconnected devices in emerging communication standards such as 6G, backscatter communication (BC) has gained traction as a promising approach for integrating the enormous amount of nodes involved [1]. Already adopted by billions of radio frequency identification (RFID) devices [2], BC enables power-efficient, low-complexity, and low-cost nodes, whereby a dedicated infrastructure is typically used. In order to omit this dedicated infrastructure to further reduce cost and complexity, ambient BC systems have been proposed [3], where the backscatter device (BD) is reflecting ambient signals, such as Wi-Fi or Long Term Evolution (LTE). These systems generally suffer from strong direct link interference (DLI) [3], demanding high dynamic range of the system's receiver to detect the backscatter (BS) signal [4]. But the possibility to obtain wideband channel state information (CSI) of the BS channel enables wireless positioning of the BD.

A crucial step in estimating the CSI of the BS channel is mitigating the DLI, which has been addressed in [2] by using purposely designed direct sequence spread spectrum (DSSS) sequences in the system transmit signal tied to the timing of the BS modulation signal. In ambient BC the waveforms are given by the ambient source, hence special waveform designs are not viable and due to the low complexity of the BD, synchronisation between the BD and the ambient source can generally not be assumed.

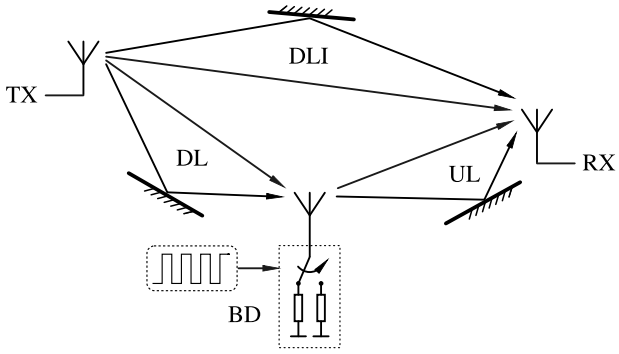

Fig. 1. Schematic system model: An OFDM signal transmitted from the TX impinges at the RX as the sum of the strong DLI with several mutlipath components and the weak BS modulated signal from the BD.

To overcome these issues, we present an algorithm which is able to estimate the unknown synchronisation parameters using generic wideband excitation signals, such as OFDM in scenarios depicted by Fig. 1. The algorithm also estimates the channel impulse response (CIR) of the DLI, cancels the DLI, and finally estimates the CIR of the BS channel.

II. Signal Model

We use a time-domain signal model that is schematically depicted in Fig. 2. A wideband transmit signal $\mathbf{s} \in \mathbb{C}^{\widetilde{N}_S \times 1}$ passes through the downlink (DL) channel $\mathbf{h}_{\mathrm{DL}} \in \mathbb{C}^{M_{\mathrm{DL}} \times 1}$ to the BD, where it is modulated with the on–off keying (OOK) signal $\mathbf{b} \in \mathbb{B}^{\mathcal{D}_{\mathrm{DL}} \times 1}$ as shown in Fig. 3, with $\mathbb{B} = \{0, 1\}$ denoting the binary set[1]. The symbol $\mathcal{D}_{\mathrm{DL}} = \widetilde{N}_S + M_{\mathrm{DL}} - 1$ denotes the dimensionality of the signal received by the BD. The signal $\mathbf{b}$ is a pulse-width modulation (PWM) signal with $50\,\%$ duty-cycle, parameterized by a start time $\eta_b \in \mathbb{N}_0$ and a period of $2T_b \in \mathbb{N}$.

[1]It can be shown that the algorithm also works for $\mathbf{b} \in \{\gamma_1, \gamma_2\}^{\mathcal{D}_{\mathrm{DL}} \times 1}$ with $\gamma_1, \gamma_2 \in \mathbb{C} \setminus \{0\}$ and $\gamma_1 \neq \gamma_2$ which may occur in practical BDs, since reflections from the BD at the constant offset in $\mathbf{b}$ (e.g. γ_1) are attributed to the direct link channel [4].

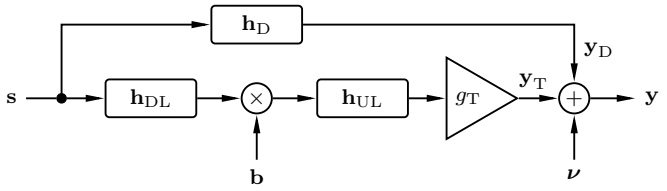

Fig. 2. Schematic overview of the time-domain signal model defined in (1).

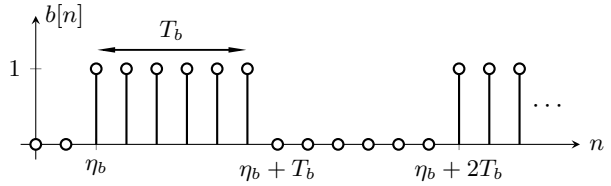

Fig. 3. Rectangular BS modulation signal with a pulse width of T_b and a start time η_b, $b[n]$ is the n-th entry of $\mathbf{b}$.

The reflected signal passes through the uplink (UL) channel $\mathbf{h}_\mathrm{UL} \in \mathbb{C}^{M_\mathrm{UL}\times 1}$ to the receiver. Level differences between DLI and received BS signal are modelled using the gain factor $g_\mathrm{T} \in (0,1)$. We assume normalized CIRs. At the receiver, the DLI $\mathbf{y}_\mathrm{D}$, i.e., $\mathbf{s}$ propagated through the direct link channel $\mathbf{h}_\mathrm{D} \in \mathbb{C}^{M_\mathrm{D}\times 1}$, is superimposing the BS signal along with zero-mean circularly-symmetric complex Gaussian noise $\boldsymbol{\nu} \in \mathbb{C}^{\mathcal{D}_\mathrm{D}\times 1}$. $\mathcal{D}_\mathrm{D} = \widetilde{N}_S + M_\mathrm{D} - 1$ denotes the length of the received signal. The received time domain signal $\mathbf{y} \in \mathbb{C}^{\mathcal{D}_\mathrm{D}\times 1}$ is

$$\mathbf{y} = \underbrace{\mathbf{H}_\mathrm{D}\mathbf{s}}_{\mathbf{y}_\mathrm{D}} + \underbrace{g_\mathrm{T}\mathbf{H}_\mathrm{UL}\mathbf{B}\mathbf{H}_\mathrm{DL}\mathbf{s}}_{\mathbf{y}_\mathrm{T}} + \boldsymbol{\nu} \tag{1}$$

where $\mathbf{H}_\mathrm{DL} \in \mathbb{C}^{\mathcal{D}_\mathrm{DL}\times \widetilde{N}_S}$, $\mathbf{H}_\mathrm{UL} \in \mathbb{C}^{\mathcal{D}_\mathrm{D}\times \mathcal{D}_\mathrm{DL}}$ and $\mathbf{H}_\mathrm{D} \in \mathbb{C}^{\mathcal{D}_\mathrm{D}\times \widetilde{N}_S}$ are Toeplitz matrices representing the linear convolutions with the corresponding CIRs $\mathbf{h}_\mathrm{DL}$, $\mathbf{h}_\mathrm{UL}$ and $\mathbf{h}_\mathrm{D}$. The BS modulation is modelled by $\mathbf{B} = \mathrm{diag}\,(\mathbf{b})$.

Additionally, we assume $\mathbf{b}$ to be narrowband compared to the CIRs (i.e., $M_\mathrm{UL} \ll T_b$), so we can approximate the BS signal with

$$\mathbf{y}_\mathrm{T} \approx g_\mathrm{T}\widetilde{\mathbf{B}}\mathbf{H}_\mathrm{UL}\mathbf{H}_\mathrm{DL}\mathbf{s} = \widetilde{\mathbf{B}}\mathbf{H}_\mathrm{T}\mathbf{s} = \widetilde{\mathbf{b}} \odot (\mathbf{S}\mathbf{h}_\mathrm{T}) \tag{2}$$

where $\odot$ denotes the Hadamard product, $\widetilde{\mathbf{b}} \in \mathbb{B}^{\mathcal{D}_\mathrm{D}\times 1}$ is $\mathbf{b}$, zero-padded to match the dimensionality of $\mathbf{y}_\mathrm{T}$ and $\widetilde{\mathbf{B}} = \mathrm{diag}\left(\widetilde{\mathbf{b}}\right)$. With this approximation, we neglect the transients to the envelope $\mathbf{b}$ caused by $\mathbf{h}_\mathrm{UL}$ in $\mathbf{y}_\mathrm{T}$. The vector $\mathbf{h}_\mathrm{T} \in \mathbb{C}^{M_\mathrm{T}\times 1}$ represents the BS CIR obtained by the linear convolution of DL and UL CIR [5]. We construct the linear convolution matrix $\mathbf{S} \in \mathbb{C}^{\mathcal{D}_\mathrm{D}\times M_\mathrm{T}}$ from $\mathbf{s}$. We further ensure $M_\mathrm{T} = M_\mathrm{DL} + M_\mathrm{UL} - 1 = M_\mathrm{D}$ by zero-padding the CIRs accordingly. We assume the transmit signal $\mathbf{s}$ to be known, e.g. by reconstruction from an OFDM transmission over the direct link. Relevant parameters used in the signal model are summarized in Table I.

III. Algorithm

In this section, we address the following problem: the CIR of the BS channel shall be estimated from a given received signal vector $\mathbf{y}$ induced by a known transmit signal $\mathbf{s}$. The challenge in this regard is removing the strong DLI interfering the weak BS signal [6], which undergoes a high attenuation inherent to BS channels [5]. A straightforward approach would be to estimate $\mathbf{h}_\mathrm{D}$ from $\mathbf{y}$ when $b[n] = 0$ and use it to reconstruct and cancel the DLI, requiring knowledge about the BS modulation parameters.

TABLE I
Parameters used in the signal model.

Parameter	Description	Domain	Known
$\mathbf{s}$	wideband transmit signal	$\mathbb{C}^{\widetilde{N}_S\times 1}$	yes
$\mathbf{y}$	received signal	$\mathbb{C}^{\mathcal{D}_\mathrm{D}\times 1}$	yes
$\boldsymbol{\nu}$	received noise	$\mathbb{C}^{\mathcal{D}_\mathrm{D}\times 1}$	no
$\mathbf{h}_\mathrm{D}$	CIR of direct link	$\mathbb{C}^{M_\mathrm{D}\times 1}$	no
$\mathbf{h}_\mathrm{DL}$	CIR of DL	$\mathbb{C}^{M_\mathrm{DL}\times 1}$	no
$\mathbf{h}_\mathrm{UL}$	CIR of UL	$\mathbb{C}^{M_\mathrm{UL}\times 1}$	no
g_T	gain of BS channel	$(0,1)$	no
η_b	start time of BS mod.	$\mathbb{N}_0$	no
T_b	pulse width of BS mod.	$\mathbb{N}$	no

In the following, we first introduce the general method used to obtain the CIRs, from which we derive an objective function with inherent DLI cancellation. Its maximisation yields the estimates of the BS modulation parameters.

A. Channel Separation and Estimation

Let us consider the likelihood function of $\mathbf{y}$ with the approximation in (2). Since $\boldsymbol{\nu} \sim \mathcal{CN}(\mathbf{0}, \sigma_\nu^2\mathbf{I})$, we get $\mathbf{y} \sim \mathcal{CN}(\mathbf{y}_\mathrm{D} + \mathbf{y}_\mathrm{T}, \sigma_\nu^2\mathbf{I})$ [7]. In order to estimate the DLI channel, we remove the dependency of $\mathbf{y}_\mathrm{T}$. An option is to transform the received signal vector according to

$$\check{\mathbf{y}} = \mathbf{A}(\eta_b, T_b)\mathbf{y} \tag{3}$$

where

$$\mathbf{A}(\eta_b, T_b) = \left[\begin{array}{c|c|c|c} \overbrace{\begin{array}{cc} 1 & 0\cdots 0 \\ 0 & \\ & 0 \\ & 1 \\ \mathbf{I}_{\eta_b} & 0 \\ & \\ 0\cdots\cdots 0 & \end{array}}^{\eta_b} & \overbrace{\begin{array}{c} 0\cdots 0 \\ \\ \\ 0\cdots 0 \\ \\ \\ 0\cdots 0 \end{array}}^{T_b} & \overbrace{\begin{array}{c} 0\cdots 0 \\ \\ \\ 0 \\ 1 \\ 0\quad 0 \\ \quad\ddots\ 1 \\ \mathbf{I}_{T_b}\ 0 \\ 0\cdots 0 \end{array}}^{T_b} & \begin{array}{c} \cdots \\ \cdots \\ \cdots \\ \cdots \\ \cdots \\ \cdots \\ \cdots \\ \cdots \\ \cdots \end{array} \end{array}\right] \tag{4}$$

is a truncation matrix parameterized by (η_b, T_b) where $\mathbf{I}_{\eta_b}$ denotes an $\eta_b \times \eta_b$ identity matrix and $\mathbf{I}_{T_b}$ denotes a $T_b \times T_b$ identity matrix. The matrix $\mathbf{A}(\eta_b, T_b)$ removes all entries from the received signal vector $\mathbf{y}$ which contain components of the BS signal, in other words, it ensures that the direct link is estimated only if the BD is not transmitting.

Assuming perfect knowledge of (η_b, T_b) characterizing (4), we obtain the likelihood

$$p(\check{\mathbf{y}}; \mathbf{h}_\mathrm{D}, \mathbf{h}_\mathrm{T}, \widetilde{\mathbf{b}}) = p(\check{\mathbf{y}}; \mathbf{h}_\mathrm{D}) \propto$$
$$\exp\left[-\left(\check{\mathbf{y}} - \mathbf{A}(\eta_b, T_b)\mathbf{S}\mathbf{h}_\mathrm{D}\right)^\mathsf{H} \boldsymbol{\Sigma}_{\nu'}^{-1} \left(\check{\mathbf{y}} - \mathbf{A}(\eta_b, T_b)\mathbf{S}\mathbf{h}_\mathrm{D}\right)\right] \tag{5}$$

which does not depend on $\mathbf{y}_\mathrm{T}$ since

$$\mathbf{A}(\eta_b, T_b)\mathbf{y}_\mathrm{T} = \mathbf{A}(\eta_b, T_b)\widetilde{\mathbf{b}} \odot (\mathbf{S}\mathbf{h}_\mathrm{T}) = \mathbf{0} \tag{6}$$

and where

$$\mathbf{\Sigma}_{\nu'} = \sigma_\nu^2 \mathbf{A}(\eta_b, T_b)\mathbf{A}^\mathsf{H}(\eta_b, T_b) = \sigma_\nu^2 \mathbf{I}. \tag{7}$$

The estimate for the direct link channel is obtained in maximum likelihood (ML) fashion

$$\hat{\mathbf{h}}_\mathrm{D} = \arg\max_{\mathbf{h}_\mathrm{D}} p(\check{\mathbf{y}}; \mathbf{h}_\mathrm{D}) = (\mathbf{A}(\eta_b, T_b)\mathbf{S})^+ \check{\mathbf{y}} \tag{8}$$

where $(\cdot)^+$ denotes the pseudoinverse. It is evident that (8) only works if we know the parameters (η_b, T_b) of the BS modulation signal, whose estimation will be addressed in the next step.

B. Backscatter Modulation Parameter Estimation

We now analyze (8) for arbitrary modulation parameters (η, T) which differ from the true parameters (η_b, T_b). At first glance, this estimator does not seem to be useful in finding the parameters of $\widetilde{\mathbf{b}}$ as it depends on them, yet it can be applied for cancelling the direct link signal, since in the noise-free case and with a truncation matrix with arbitrary parameters we get

$$\hat{\mathbf{h}}_\mathrm{D} = \mathbf{h}_\mathrm{D} + \mathbf{L}(\eta, T)\mathbf{h}_\mathrm{T} \tag{9}$$

where

$$\mathbf{L}(\eta, T) = (\mathbf{A}(\eta, T)\mathbf{S})^+ \mathbf{A}(\eta, T)\widetilde{\mathbf{B}}\mathbf{S} \tag{10}$$

is a leakage matrix of dimension $M_\mathrm{D} \times M_\mathrm{T}$ which does not depend on $\mathbf{h}_\mathrm{D}$. With this finding, we can construct the residual $\bar{\mathbf{y}}$ for the noise-free case, which is

$$\begin{aligned}\bar{\mathbf{y}} &= \mathbf{y} - \mathbf{S}\hat{\mathbf{h}}_\mathrm{D} = \mathbf{y}_\mathrm{D} + \mathbf{y}_\mathrm{T} - \mathbf{S}\hat{\mathbf{h}}_\mathrm{D} \\ &= \mathbf{y}_\mathrm{D} + \mathbf{y}_\mathrm{T} - \underbrace{\mathbf{S}\mathbf{h}_\mathrm{D}}_{\mathbf{y}_\mathrm{D}} - \mathbf{S}\mathbf{L}(\eta, T)\mathbf{h}_\mathrm{T} = \mathbf{y}_\mathrm{T} - \mathbf{S}\mathbf{L}(\eta, T)\mathbf{h}_\mathrm{T}\end{aligned} \tag{11}$$

where any influence of the direct link channel is eliminated. A crucial property of $\mathbf{L}(\eta, T)$ is that it approaches zero if we approach the true parameters of the BS modulation signal $\widetilde{\mathbf{b}}$, i.e. $\mathbf{L}(\eta, T) \to \mathbf{0}$ for $(\eta, T) \to (\eta_b, T_b)$, which is equivalent to maximizing the energy of the residual $\bar{\mathbf{y}}$. By inserting (3) and (8), we obtain the estimator

$$\begin{aligned}(\hat{\eta}_b, \hat{T}_b) = \arg\max_{\eta, T} J(\eta, T) = \arg\max_{\eta, T} \|\bar{\mathbf{y}}\|^2 = \\ \arg\max_{\eta, T} \left\| \left(\mathbf{I} - \mathbf{S} \left(\mathbf{A}(\eta, T)\mathbf{S} \right)^+ \mathbf{A}(\eta, T) \right) \mathbf{y} \right\|^2.\end{aligned} \tag{12}$$

Since (12) is a nonlinear integer optimization problem, we employ a grid search over a sensible set of parameters η_b and T_b which are of practical relevance. The implementation is summarized by Algorithm 1.

Now, having the parameters of $\widetilde{\mathbf{b}}$, we can reapply the estimator in (8) with the estimated parameters $(\hat{\eta}_b, \hat{T}_b)$ to obtain $\hat{\mathbf{h}}_\mathrm{D}$, which we use to perform the final interference cancellation by reconstructing and cancelling the DLI to get estimate of the BS signal

$$\hat{\mathbf{y}}_\mathrm{T} = \mathbf{y} - \mathbf{S}\hat{\mathbf{h}}_\mathrm{D}. \tag{13}$$

The BS CIR is obtained in analogous fashion to (8), resulting in

$$\hat{\mathbf{h}}_\mathrm{T} = \left(\mathbf{B}(\hat{\eta}_b, \hat{T}_b)\mathbf{S} \right)^+ \mathbf{B}(\hat{\eta}_b, \hat{T}_b)\hat{\mathbf{y}}_\mathrm{T} \tag{14}$$

where $\mathbf{B}(\hat{\eta}, \hat{T})$ is the truncation matrix derived from the estimated BS modulation signal, removing all entries from $\hat{\mathbf{y}}_\mathrm{T}$ where no reflection of the BD is present. The matrix $\mathbf{B}(\hat{\eta}, \hat{T})$ is the complementary transformation to $\mathbf{A}(\hat{\eta}, \hat{T})$.

Algorithm 1: BS modulation signal parameter estimation.

Require: modulation start times $\{\eta_i\}_{i=1}^{N_\eta}$, modulation pulse widths $\{T_j\}_{j=1}^{N_T}$, transmit signal $\mathbf{s}$, received signal $\mathbf{y}$
  $\mathbf{S} \leftarrow$ `convmtx`$(\mathbf{s})$; `// conv. matrix from TX signal`
  for all η_i, T_j **do**
    $\mathbf{A}(\eta_i, T_j) \leftarrow$ `truncmtx`(η_i, T_j); `// Equation (4)`
    $\check{\mathbf{y}} \leftarrow \mathbf{A}(\eta_i, T_j)\mathbf{y}$; `// Equation (3)`
    $\hat{\mathbf{h}}_\mathrm{D} \leftarrow (\mathbf{A}(\eta_i, T_j)\mathbf{S})^+ \check{\mathbf{y}}$; `// Equation (8)`
    $\bar{\mathbf{y}} \leftarrow \mathbf{y} - \mathbf{S}\hat{\mathbf{h}}_\mathrm{D}$; `// Equation (13)`
    $J(\eta_i, T_j) \leftarrow \|\bar{\mathbf{y}}\|^2$
  end for
  $(\hat{\eta}, \hat{T}) \leftarrow \arg\max J(\eta_i, T_j)$; `// Equation (12)`
Ensure: $\hat{\eta}$, $\hat{T}$

IV. Evaluation

A. Simulation

The algorithm is evaluated using a standard-compliant OFDM signal. Sample rate f_s, subcarrier count N_c, and subcarrier spacing of the transmit signal are defined by an IEEE 802.11ax transmission mode operating at $f_\mathrm{c} = 2.44\,\mathrm{GHz}$ with $80\,\mathrm{MHz}$ bandwidth. The BS modulation signal is based on an FM0 Extended Preamble defined in the Electronic Product Code (EPC) Class 1 Gen 2 RFID standard [8], which corresponds to a $40\,\mathrm{kHz}$ and $50\,\%$ duty-cycle PWM signal with a total duration of $300\,\mu\mathrm{s}$. The dimensionality of the transmit signal $\mathbf{s}$ and the received signal $\mathbf{y}$ are set such that it matches the duration of the BS modulation preamble with the given sample period.

The received signal $\mathbf{y}$ is synthesized using the signal model in (1) without the approximation in (2). We first apply (12) to get the BS modulation parameters. Next, the direct link CIR is estimated using (8) to perform DLI cancellation according to (13). Finally, we get the estimate of the BS CIR by applying (14) to the residual received signal after DLI cancellation.

In order to evaluate the performance of the algorithm, we employ Monte Carlo (MC) simulations for different combinations of interference-to-noise ratios (INRs) (i.e. the signal-

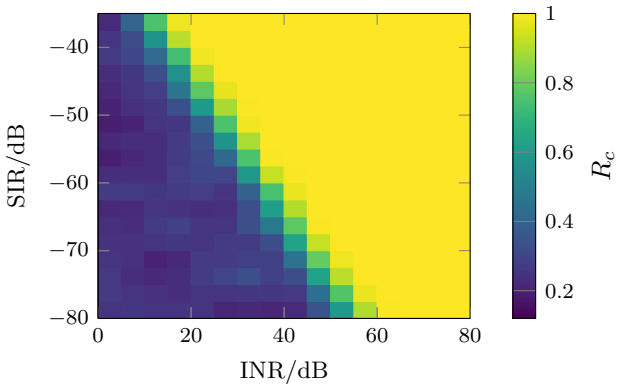

Fig. 4. Rate of correct estimation of BS modulation parameters for different combinations of INR and SIR.

to-noise ratio (SNR) of the OFDM signal) and signal-to-interference ratios (SIRs),

$$\mathrm{INR} = 10\log\frac{1}{N_c\sigma_\nu^2}, \tag{15}$$

$$\mathrm{SIR} = 20\log g_\mathrm{T}. \tag{16}$$

For each experiment, the BS modulation start time η_b is drawn from a discrete uniform distribution $\mathcal{U}(0, T_b)$ and the CIRs are randomly generated. To characterize the performance of the estimator of the BS modulation parameters in (12), we define the rate of correct estimation in (17), where $e_\eta = \eta_b - \hat{\eta}_b$, $e_f = f - \hat{f}$ with $f = \frac{f_s}{2T_b}$, $\Delta_\eta = 100$ and $\Delta_f = 1\,\mathrm{kHz}$ define the spacing of the grid. By

$$R_c = \mathbb{P}\left[|e_\eta| < \Delta_\eta \cap |e_f| < \Delta_f\right] \tag{17}$$

we denote the probability that the start time and frequency of the BS modulation signal are correctly estimated with grid-spacing accuracy. Fig. 4 shows the simulated results for R_c, where we can see at first glance that for the given setup, the SNR of the BS signal $\mathrm{SNR}_{\mathbf{y}_\mathrm{T}} = \mathrm{INR}+\mathrm{SIR}$ needs to be above $-20\,\mathrm{dB}$ such that the estimation in (12) performs reliably.

To characterize the performance of the full system, we use the SNR of the BS CIR defined in (18). It corresponds to the ratio of energy in $\mathbf{h}_\mathrm{T}$ to the error energy per signal dimension.

$$\mathrm{SNR}_{\mathbf{h}_\mathrm{T}} = 10\log\frac{\|\mathbf{h}_\mathrm{T}\|^2 M_\mathrm{T}}{\mathbb{E}\left[\|\mathbf{h}_\mathrm{T} - \hat{\mathbf{h}}_\mathrm{T}\|^2\right]} \tag{18}$$

Fig. 5 shows the simulated $\mathrm{SNR}_{\mathbf{h}_\mathrm{T}}$ for different SIR values. For low INR values, the $\mathrm{SNR}_{\mathbf{h}_\mathrm{T}}$ is dominated by noise, additionally, separation of the channels is not possible since (12) is not performing well, resulting in a non-zero leakage matrix $\mathbf{L}(\eta, T)$, potentially also cancelling the BS channel in (13). In the region where (12) starts to produce reliable results, we can observe a slightly steeper slope. Further increasing the INR, we can see that the $\mathrm{SNR}_{\mathbf{h}_\mathrm{T}}$ is driven into saturation and does no longer increase. This behaviour is likely caused by the approximation in (2) but would require further investigation. $\hat{\mathbf{h}}_\mathrm{T}$ starts to produce reliable results for $\mathrm{SNR}_{\mathbf{h}_\mathrm{T}} > 20\,\mathrm{dB}$, i.e. in the region where $R_c = 1$. For data detection, one can use this $\hat{\mathbf{h}}_\mathrm{T}$ to accumulate the energy of the BS symbols. Each

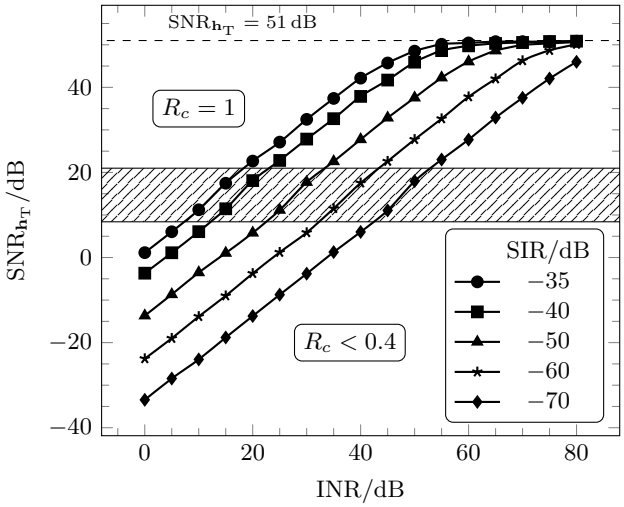

Fig. 5. SNR of the estimated BS channel $\hat{\mathbf{h}}_\mathrm{T}$ for different SIR values. The hatched area indicates the region where the estimator of the BS modulation parameters starts to produce reliable results. For increasing INR values, the SNR settles in at 51 dB.

cycle of the BS signal (i.e. one FM0 symbol or one cycle of a Miller subcarrier sequence [8]) then yields roughly 11 dB less SNR at the accumulator output, because the periodic preamble comprises 12 cycles in our example.

B. Measurement

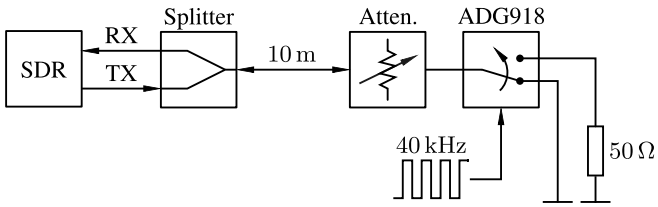

Fig. 6. Wired setup for bistatic BS measurement using an SDR. The USRP is connected to a *HUBER+SUHNER 4901.19.A* resistive splitter with two 1 m long coaxial cables. Signals in the BS path are attenuated by a *Keysight 8494B*. The PWM switching signal is generated by a *Keysight 33522B*.

A proof-of-concept measurement is performed using the wired BS setup in Fig. 6. We implement an SDR wideband transceiver using an X410 USRP from *National Instruments*, controlled by a host-PC running GNU Radio. The TX signal of the USRP is split up in two paths, one is directly routed back to an RX port of the USRP (forming the direct link) and the remaining one is dedicated to the BD. The BD is connected to the splitter using a 10 m long coaxial cable to introduce a significant propagation delay, useful to obtain CIRs which can easily be distinguished from the direct path, to see at first glance whether the algorithm works. Additionally, we insert a variable RF attenuator to set the SIR of the BS channel. For the BD, we use an ADG918 CMOS-based RF switch from *Analog Devices*, which has already been successfully used in [9] for a similar experiment. An evaluation board of the ADG918 is used along with external impedances, chosen to obtain the behaviour of the BD described by Fig. 3. The PWM switching signal is produced by an arbitrary waveform generator.

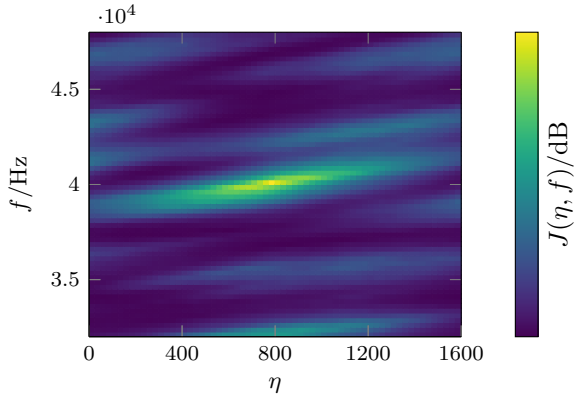

Fig. 7. The objective function $J(\eta, f)$ from (12) for modulation parameter estimation evaluated on measured data, peaking at the set modulation frequency of 40 kHz.

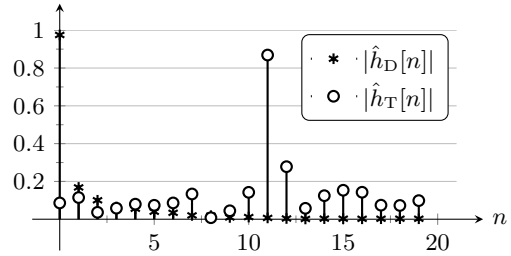

Fig. 8. Estimated normalized CIRs of the cabled measurement setup using (8) for $\hat{\mathbf{h}}_{\mathrm{D}}$ and (14) for $\hat{\mathbf{h}}_{\mathrm{T}}$. One sample in the delay domain corresponds to a distance of roughly 2 m with the sample frequency and cable used. The peak in $\hat{\mathbf{h}}_{\mathrm{T}}$ coincides with the expected roundtrip distance of roughly 20 m.

The baseband transmit signal $\mathbf{s}$ is a known pseudo-noise vector where $s[n] \overset{\text{i.i.d.}}{\sim} \mathcal{CN}(0.25 + 0.25j, 0.1^2)$. The sample frequency of the transceiver is set to $f_s = 122.88\,\mathrm{MHz}$ and the carrier frequency is set to $f_c = 2.44\,\mathrm{GHz}$. The total duration of the received signal, i.e., $\dim(\mathbf{y})$, is again chosen to match the full length of the BS preamble (we use the same BS modulation signal as for the simulation). The RF attenuator is set such that $\mathrm{SIR} \approx -40\,\mathrm{dB}$ including losses of the cables, losses of the splitter and the insertion loss of the ADG918 during reflection.

To the received baseband signal $\mathbf{y}$ from the USRP we first apply (12) to obtain the BS modulation parameters. The resulting objective function for the measured data is displayed in Fig. 7, peaking at the expected modulation frequency of $f = \frac{f_s}{2T} = 40\,\mathrm{kHz}$.

Next, we estimate the CIR of the direct link using (8) and perform a DLI cancellation using (13). Finally, we apply (14) to obtain the CIR of the BS channel. The normalized results of the CIRs are shown in Fig. 8, where for the BS channel we get an expected peak at a delay roughly corresponding to twice the cable length, indicating correct functioning of the algorithm.

V. Conclusion

We introduced an approach for estimating the unknown parameters of the BS modulation signal in a bistatic BS scenario with strong DLI using generic wideband excitation signals. The obtained parameters are subsequently used to separate the BS signal from the DLI to estimate the CSI of the BS channel, enabling the positioning of the BD. The obtained algorithm is evaluated by means of a simulation using a standard OFDM transmit signal along with an RFID preamble for the BS modulation. It has been shown that the parameters of the BS modulation are successfully recovered in a low-SNR regime of $-20\,\mathrm{dB}$. Additionally, we performed a proof-of-concept measurement using an SDR and successfully validated the algorithm.

Acknowledgment

The financial support by the Christian Doppler Research Association and the European Union's Horizon 2020 program (grant agreement No 101013425) is gratefully acknowledged.

References

[1] I. F. Akyildiz, A. Kak, and S. Nie, "6G and beyond: The future of wireless communications systems," *IEEE Access*, vol. 8, pp. 133 995–134 030, 2020. DOI: 10.1109/ACCESS.2020.3010896.

[2] H. Arthaber, T. Faseth, and F. Galler, "Spread-spectrum based ranging of passive UHF EPC RFID tags," *IEEE Commun. Lett.*, vol. 19, no. 10, pp. 1734–1737, 2015. DOI: 10.1109/LCOMM.2015.2469664.

[3] N. Van Huynh, D. T. Hoang, X. Lu, D. Niyato, P. Wang, and D. I. Kim, "Ambient backscatter communications: A contemporary survey," *IEEE Commun. Surveys Tuts.*, vol. 20, no. 4, pp. 2889–2922, 2018. DOI: 10.1109/COMST.2018.2841964.

[4] A. Kaplan, J. Vieira, and E. G. Larsson, "Direct link interference suppression for bistatic backscatter communication in distributed MIMO," *IEEE Trans. Wireless Commun.*, vol. 23, no. 2, pp. 1024–1036, 2024. DOI: 10.1109/TWC.2023.3285250.

[5] D. Arnitz, U. Muehlmann, and K. Witrisal, "Wideband characterization of backscatter channels," in *17th European Wireless 2011 - Sustainable Wireless Technologies*, 2011, pp. 1–7.

[6] D. Arnitz, U. Muehlmann, and K. Witrisal, "Characterization and modeling of UHF RFID channels for ranging and localization," *IEEE Trans. Antennas Propag.*, vol. 60, no. 5, pp. 2491–2501, 2012. DOI: 10.1109/TAP.2012.2189705.

[7] S. M. Kay, *Fundamentals of Statistical Signal Processing: Estimation Theory* (Prentice-Hall signal processing series). Englewood Cliffs, N.J.: PTR Prentice-Hall, 1993, ISBN: 0133457117.

[8] GS1, "EPC UHF Gen2 air interface protocol," GS1, Avenue Louise 326, 1050 Brussels, Belgium, Standard, 2024. [Online]. Available: https://www.gs1.org/standards/rfid/uhf-air-interface-protocol.

[9] J. F. Ensworth and M. S. Reynolds, "BLE-backscatter: Ultralow-power IoT nodes compatible with Bluetooth 4.0 low energy (BLE) smartphones and tablets," *IEEE Trans. Microw. Theory Tech.*, vol. 65, no. 9, pp. 3360–3368, 2017. DOI: 10.1109/TMTT.2017.2687866.